ACS Sustainable Resource Management

pubs.acs.org/acssrm

Article

Crosslinked Polyethyleneimine Networks for Rapid and Selective Gold Recovery from Electronic Waste

Syfur R. Tushar, Yong Li, James Murowchick, Todor Gounev, Nafisa Tasnim, Sai Siva Kumar Pinnepalli,[#] Peng Tao,* Zhonghua Peng,* and Xiaobo Chen*

Cite This: *ACS Sustain. Resour. Manag.* 2026, 3, 1182−1191

Read Online

ACCESS | Metrics & More | Article Recommendations | Supporting Information

ABSTRACT: Electronic waste, or e-waste, is one of the fastest-growing waste streams as electronic gadgets become increasingly prevalent and short-lived. E-waste contains a significant amount of precious metal gold (Au), whose retrieval offers substantial financial and environmental benefits. We have previously developed triazine-crosslinked polyethyleneimines (TCPEIs) that can capture Au(III) with high capacity, high selectivity, and fast kinetics. Herein, to better understand the underlying mechanisms, we studied the gold adsorption on crosslinked polyethyleneimines (CPEIs) with rigid crosslinkers of varying lengths and a different PEI type. Specifically, a triazine (2,4,6-trichloro triazine, TCT) and a piperazine-bridged triazine dimer (1,4-di(4,6-dichloro-1,3,5-triazine-2-yl)piperazine, DTP) were used to crosslink linear PEIs to generate CPEIs − lTCPEI and lDCPEI, respectively. lDCPEI, with a longer rigid crosslinker, consistently showed faster adsorption kinetics across all three tested initial gold concentrations than lTCPEI, and the lower the gold concentration, the more pronounced the difference in their adsorption rates. At 20 ppm, a gold concentration that is relevant to the acidic leaching solution of electronic waste, lDCPEI exhibited a gold adsorption rate constant ($K_2 = 0.5837$ g mg^{-1} min^{-1}) that is more than twice as high as that of lTCPEI ($K_2 = 0.2231$ g mg^{-1} min^{-1}). The gold recovery efficiency of lDCPEI is also significantly higher than that of lTCPEI at this concentration. The maximum adsorption capacities of the lDCPEI and lTCPEI as determined by Langmuir isotherm analysis are, however, comparable, and are 2777 and 2857 mg g^{-1}, respectively. X-ray diffraction analysis indicated that the predominant mechanism of initial adsorption is electrostatic interactions, followed by the reduction of Au(III) ions. In the presence of competing metal ions of even higher concentrations, lDCPEI was able to recover 99% of the gold. Moreover, the desorption study showed that 99% of the adsorbed gold could be recovered within 30 s. This simple approach to e-waste recycling offers sustainable benefits for both the circular economy and environmental protection.

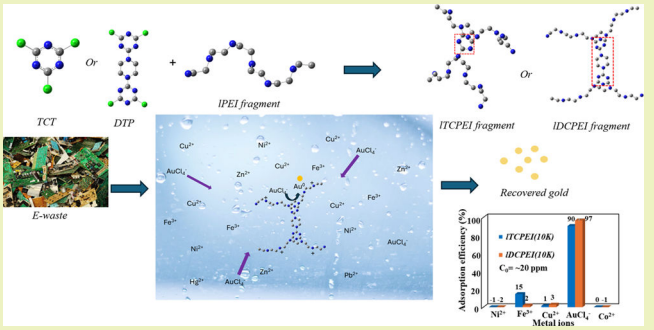

KEYWORDS: *e-waste, gold retrieval, crosslinked polyethyleneimine, waste water, metal recovery, green chemistry*

1. INTRODUCTION

Electronic waste (e-waste) is considered one of the fastest-growing solid waste streams worldwide and poses a significant hazard to human health and the environment.[1,2] The rapidly growing economy and evolving technology, as well as customer demands for improved functionality and design, have reduced the lifespan of electronics and resulted in a significant increase in e-waste generation. In 2022, a record 62 million metric tons of e-waste were generated, and it is estimated that it will be about 82 million metric tons in 2030.[3] Despite e-waste generation increasing 3–5% every year, only 22.3% was recycled in 2022, with reports predicting that it will further decline in the near future.[3,4] The major components of e-waste materials include 60.2% metals, 15.2% plastics, 5% metal-plastic mixtures, and 1.7% printed circuit boards.[5] E-waste approximately contains 60 different metals, including precious metals like gold, silver, and palladium, and other valuable metals like copper, aluminum, and iron. It also consists of extremely toxic metals such as lead, mercury, and cadmium, as well as the metalloid arsenic.[6,7] As a result, releasing e-waste to the environment poses a severe risk to human health and the environment.[8,9] Recovering valuable metals from e-waste can help create a circular economy, protect the environment and provide financial benefits.[10] Recycling from e-waste is getting popular due to precious metals such as gold, making it profitable.[11]

Received: January 9, 2026
Revised: March 20, 2026
Accepted: March 23, 2026
Published: March 31, 2026

Gold is precious due to its intrinsic value and scarcity, as well as its aesthetic qualities, historically serving as a core component of hard currency.[12] However, demand for gold in electronics has increased significantly due to its unique physical and chemical properties.[13] Gold is a very efficient conductor of electricity, and resistant to corrosion, making gold based electronic devices highly reliable.[14] It is widely used in electronic devices such as connectors, switches, hybrid circuits, soldered joints, connecting wires, and connection strips.[15] As gold is wildly used in electronics, the e-waste now contains significant amounts of gold along with other metals. The concentration of gold may vary considerably depending on the sources of e-waste ranging from 10 to 1600 ppm.[4] A typical rich gold-containing ore's gold concentration is about 18 ppm, whereas the average gold concentration in e-waste is much higher.[4]

The global e-waste precious metal recovery market reached 5.9 billion US dollars in 2023, with gold accounting for ∼70% of the total value.[16] Recycled gold from e-waste also helps to meet global demand, which reduces expensive and environmentally harmful gold mining and extraction operations. Commonly used approaches for gold recovery include precipitation,[17] ion exchange,[18] solvent extraction,[19] and membrane separation.[20] However, such methods often lack sufficient selectivity and high capacitity.[21] Adsorption, on the other hand, can be efficient, cost-effective, and eco-friendly.[22] Recent progress in polyethyleneimines (PEI)-based adsorbents has focused on structural modification to improve Au uptake and selectivity.[23,24] Crosslinking PEI or incorporating it into composite PEI to form a porous and water insoluble structure is an example of some attractive strategy.[25,26] Despite these advances, direct, systematic control of network openness via linker length in PEI systems has not been emphasized. Indeed, we have recently shown that branched polyethyleneimines (bPEIs) crosslinked with rigid 2,4,6-trichloro-1,3,5-triazine (TCT) led to crosslinked PEI networks that showed remarkably high adsorption capacity and fast adsorption kinetics toward the $[AuCl_4]^-$ anion.[27]

The rigid nature of the TCT crosslinker is thought to play a central role in forming a crosslinked network with open and accessible pores which are responsible for the fast adsorption rate. We speculate that the openness of the network's pores may depend on the length of the rigid crosslinker and a longer crosslinker may further expand and open up the pores, leading to CPEI-based networks with even faster adsorption rates and capacities. To test this hypothesis, a new crosslinker, 1,4-di(4,6-dichloro-1,3,5-triazine-2-yl)piperazine (DTP) of similar rigidity but tripled in length of TCT was synthesized. Linear PEI (lPEI) instead of bPEI was used due to its uniform structure and the presence of predominantly secondary amine groups along the straight polymer chain which are known to be rather reactive with TCT. This uniform linear chain allows us to create well-defined uniform pore structures after crosslinking with a rigid crosslinker, where the size of the pores will be fully dictated by the size of the crosslinker. With two rigid crosslinkers of significantly different sizes and two linear PEIs of different molecular weights (10 and 1.8 kDa, respectively), a series of crosslinked polymers, namely, TCT-crosslinked lPEI (lTCPEI) and DTP-crosslinked lPEI (lDCPEI), were synthesized. The gold adsorption kinetics of these two types of adsorbents were comparatively studied, and it was found that lDCPEI is indeed faster than TCPEI toward $[AuCl_4]^-$ adsorption. Kinetics data were fitted to the pseudo-second-order adsorption kinetics models, showing that the adsorption rate (K_2) for lDCPEI was around two times faster than that of lTCPEI. Gold adsorbed on lDCPEI can be desorbed almost 100% within 30 s (s) using thiourea. CPEIs exposed to $[AuCl_4]^-$ solutions for different amounts of time and subsequently separated from the solution and then stored for different extended period of time were thoroughly examined with X-ray diffraction (XRD), Fourier-transform infrared (FTIR) spectroscopy, and scanning electron microscopy (SEM). Initial adsorption of $[AuCl_4]^-$ appears to be driven by electrostatic attraction between positively charged PEIs and the negatively charged $[AuCl_4]^-$ complex. A redox reaction that involves the reduction of Au(III) to metal Au(0) by amines in PEI follows and may last for days. Gold absorbed on CPEIs, however, whether in the complex form or as metal Au(0), can be desorbed by thiourea while regenerating CPEIs. These results provide valuable insights into the gold recovery industry and advance our understanding of the chemistry of amine-gold complexes.

2. MATERIALS AND METHODS

2.1. Materials

Two linear polyethyleneimines (lPEI, Mn 10,000 Da, purity: >99.0%, and Mn 1800 Da, purity: >99.0%) were obtained from GLPBIO Technology, USA. 2,4,6-Trichloro-1,3,5-triazine (TCT, 99%) was purchased from Sigma Aldrich. Tetrahydrofuran (THF, 99%), dimethylformamide (DMF, 99%), and chloroform (99%) were provided by Fisher Scientific, USA. Gold chloride trihydrate (99.9%) and piperazine (99%) were bought from Sigma Aldrich, USA. Potassium hexacyanocobaltate(III) (99%) was bought from Millipore Sigma, USA. All the reagents were of analytical grade and used without further purification, except for THF, which was dried with 3 Å molecular sieves overnight before use.

2.2. Analytical Instrumentation

Atomic absorption spectroscopy (AAS, model: Agilent 55) was used to determine the concentration of metal ions in solution. ^{13}C solid-state magic-angle spinning (MAS) nuclear magnetic resonance (NMR) spectra were acquired on a Varian spectrometer equipped with an 8.5 T wide-bore magnet at a Larmor frequency of 89.822 MHz and MAS frequency of 7 kHz with 40k transients. FTIR was conducted with a Shimadzu IRAffinity-1 spectrophotometer in the range of 500–4000 cm^{-1} at room temperature. XRD analysis was carried out using a Rigaku Miniflex 600C X-Ray diffractometer over a 2θ range of 5–85 degrees using Cu Kα radiation. and EDS studies were carried out with Tescan Vega 3 LMU and Bruker Quantax EDS instruments, respectively.

2.3. Synthesis of Crosslinked Polymers

To evaluate the effect of the crosslinker size, two crosslinkers, a smaller and rigid 2,4,6-trichloro-1,3,5-triazine (TCT) and a larger and rigid 1,4-di(4,6-dichloro-1,3,5-triazine-2-yl)piperazine (DTP), which is approximately three times in length were selected (SI-1). Two linear polyethyleneimines (lPEIs) with significantly different molecular weights (10 and 1.8 kDa) were crosslinked with these crosslinkers to assess the effect of the size of lPEI.

2.3.1. Synthesis of lTCPEIs. TCT-crosslinked polyethyleneimines (TCPEIs) were synthesized following a previously published synthetic procedure with slight modifications in the washing procedure.[27] A 250-mL three-necked round-bottom flask was equipped with a magnetic stir bar and a reflux condenser. 10.48 g (1.048 mmol) of lPEI (10 kDa) and 30.0 mL of *N*,*N*-dimethylformamide (DMF) were added to the flask. The resulting mixture was stirred at room temperature for 1.5 h, followed by the dropwise addition of 2.49 g (13.5 mmol) of TCT in 10 mL of dry tetrahydrofuran (THF) through an addition funnel. The reaction mixture was subsequently stirred at 70 °C for 36 h. After being cooled to

https://doi.org/10.1021/acssusresmgt.6c00020
ACS Sustain. Resour. Manag. 2026, 3, 1182–1191

room temperature, the precipitates were collected by filtration, washed sequentially with DMF, distilled water, and then twice with acetone. The solids were then dried overnight under vacuum at room temperature. The yields for lTCPEI(10K) and lTCPEI(1.8K) are over 80%. Both polymers are light-yellow powders.

2.3.2. Synthesis of DTP. To synthesize DCPEIs, a new crosslinker DTP was first synthesized from TCT and piperazine. 10.2 g (55.3 mmol) of TCT was dissolved in 75 mL of chloroform in a 250-mL two-necked round-bottom flask. The solution was cooled in an ice-water bath for 10 min under a nitrogen atmosphere. In another flask, 2.39 g (27.7 mmol) of piperazine was dissolved in 5 mL of chloroform, followed by the addition of 50 mL of *N*,*N*-diisopropyl ethylamine (DiPEA). It was then added dropwise to the TCT solution while maintaining the ice-water bath condition. The resulting solution was continuously stirred at 0 °C for 2 h. The precipitates were collected by filtration and washed twice with chloroform. The solid product was dried overnight under vacuum at room temperature. 7.62 g of DTP was obtained as light-yellow solids with a yield of 72%.

2.3.3. Synthesis of lDCPEIs. 10.98 g (1.098 mmol) of lPEI (10 kDa) was dissolved in 30.0 mL of DMF in a 250-mL three-necked round-bottom flask after continuous stirring for 1.5 h. In another flask, 4.05 g (10.60 mmol) of DTP was dissolved in 30 mL of DMF at 70 °C. This DTP solution was then added dropwise to the lPEI solution under stirring at 70 °C. The resulting reaction mixture was refluxed for another 36 h. After being cooled to room temperature, the solid precipitates were collected by filtration, washed with DMF, water, and then twice with acetone. The final product was dried in a vacuum oven overnight at room temperature. Both lDCPEI(10K) and lDCPEI(1.8K) were obtained as light-yellow powders with over 80% yields.

3. RESULTS AND DISCUSSION

3.1. Synthesis and Structural Characterization

The synthetic scheme for lTCPEI is given in the Supporting Information (SI-2). The reaction was carried out using chlorine to amine reactive functional group ratio of 1:6, following a reported protocol.[27] The crosslinking proceeds through a stepwise nucleophilic aromatic substitution reaction (S_NAr), and at 70 °C, all three chloride groups of the TCT ring have sufficient reactivity and can all undergo substituion.[28] A light-yellow solid began to precipitate shortly after two reactants were mixed at 70 °C, and after further reacting for 36 h, the resulting product was completely insoluble in water. lDCPEIs was synthesized in two steps (Scheme 1). First, the crosslinker, DTP was synthesized by reacting piperazine with TCT at 0 °C using a 1:2 piperazine to TCT molar ratio.[29] At this temperature, only one chlorine in TCT can undergo substitution, leading to the formation of a larger crosslinker, DTP. Then, PEI was crosslinked with DTP while maintaining the same chlorine to amine ratio (1:6) as lTCPEI. The reaction temperature and duration were kept the same as in the lTCPEI synthesis, and it also produced a light-yellow, water-insoluble solid. In this reaction, primary and secondary amines of the PEI backbone act as nucleophiles and attack the carbon of the triazine ring, forming covalent triazine-amine (C–N) linkages. Repetition of these substitutions on multiple triazine sites creates a three-dimensional, crosslinked polymer network. Both DTP and TCT are rigid crosslinkers, but DTP is roughly three times larger in size, which is expected to introduce larger pores in the resulting polymer networks and increase the accessibility of nitrogen binding sites.

Scheme 1. Synthesis of DTP Crosslinked lPEIs (lDCPEIs)

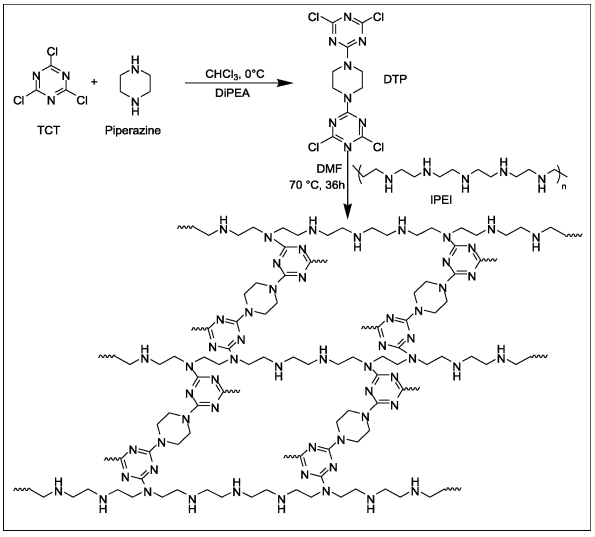

To elucidate the chemical structure of the as-synthesized crosslinked polymers, we performed ^{13}C solid-state NMR and FTIR. The ^{13}C solid-state NMR of PEI showed four distinct peaks in the range of 30–60 ppm, while TCPEI and DCEPI showed a broad peak from 30 to 65 ppm for C−N carbons which is consistent with their highly crosslinked structure. The aromatic carbon of the triazine ring, bonded with nitrogen, appeared at a chemical shift of 165–170 ppm (SI-3).[30] Figure 1 shows the FTIR spectroscopy results for the crosslinked polymers and their starting reagents. The N−H bending peak at 1652 cm^{-1} becomes more prominent in the crosslinked PEI, likely because the number of N−H bonds decreases, reducing the potential for hydrogen bonding. The aromatic ring of trichloro triazine exhibits C=N peaks near 1466 cm^{-1}.[31] These peaks are also seen in all the crosslinked polymers but shifted to higher wavenumbers due to the substitution reaction of the aromatic ring, confirming the successful crosslinking and the presence of the triazine rings within the polymers. The spectra for PEI display a broad peak around 3393 cm^{-1} due to the N−H stretching and two peaks between 2845 and 2945 cm^{-1} corresponding to the C−H stretching (SI-4).[30] These peaks also appear in all the crosslinked polymers, lTCPEIs and lDCPEIs, indicating that PEI is present in the final products (SI-4). In the case of DTP, the disappearance of the N−H stretching peak at 3213 cm^{-1} and the N−H wagging peak at 834 cm^{-1} confirms the formation of the C−N bond between TCT and the piperazine ring. The DTP also shows aromatic C=N peaks at 1560 cm^{-1}, and two intense peaks at 1238 and 987 cm^{-1} assignable to two types of the C−N stretching. These peaks are also present in lDCPEI, confirming the presence of DTP as a crosslinker. Additionally, the disappearance of the C−Cl stretching peak at 841 and 790 cm^{-1} in lTCPEI and lDCPEI spectra indicates a complete substitution of the chlorine atoms in both TCT and DTP with amines.[32,33]

3.2. Gold Adsorption Studies

3.2.1. Effect of Crosslinker Sizes on Adsorption. The adsorption capacity and efficiency of DCPEIs and TCPEIs were evaluated at different time points to investigate the effect of crosslinker sizes on adsorption. Four crosslinked polymers, lDCPEI(10K), lDCPEI(1.8K), lTCPEI(10K), and

https://doi.org/10.1021/acssusresmgt.6c00020
ACS Sustain. Resour. Manag. 2026, 3, 1182−1191

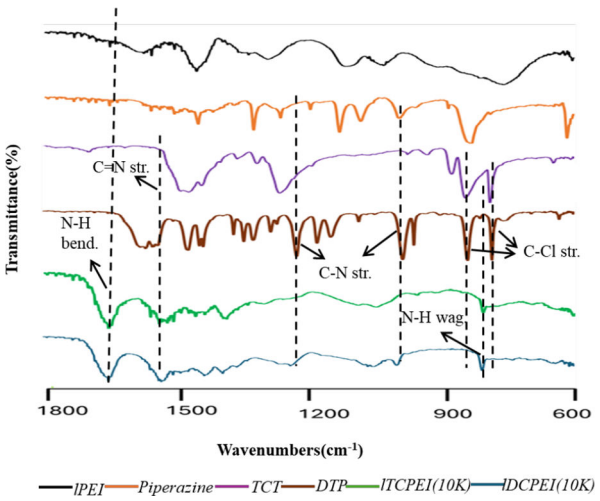

Figure 1. FTIR spectra of the CPEIs(10K) and their starting materials.

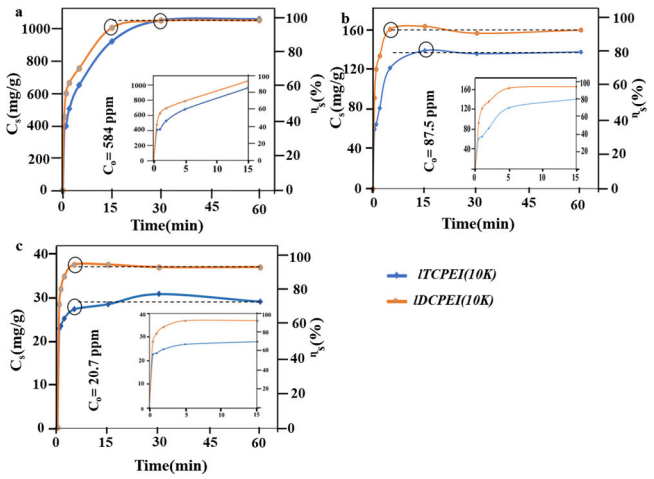

Figure 2. Comparison of adsorption capacity (C_s) and adsorption efficiency (η_s) over time (min) for lDCPEI(10K) and lTCPEI(10K) at an initial gold concentration of (a) 584, (b) 87.5, and (c) 20.7 ppm. The insets highlight comparisons for the initial 15 min for enhanced clarity. (Dashed line drawn from the final data point and circles indicate equilibrium points).

lTCPEI(1.8K), were employed as adsorbents. Since gold concentrations in e-waste can vary widely depending on its sources, we selected three different initial gold concentrations (~584, ~87, and ~20 ppm) to evaluate the performance of the adsorbents. First, the performance of lDCPEI(10K) and lTCPEI(10K) was compared at an initial gold solution concentration of 584 ppm where both adsorbents provided excess binding sites than the amount of gold present (Figure 2a). At this concentration, both lTCPEI(10K) and lDCPEI(10K) captured most of the gold from the solution and reached a 98% recovery efficiency after 60 min. Although at equilibrium both polymers exhibited similar adsorption capacity, lDCPEI(10K) consistently demonstrated slightly higher uptake and removal efficiency during the first 15 min, but the difference between the two remained modest (Figure 2a, inset). Then, the initial gold concentration was set to 87.5 and 20.7 ppm and similar experiments were carried out (Figure 2b,c). At both concentrations, lDCPEI(10K) consistently outperformed lTCPEI(10K) significantly in terms of adsorption capacity and efficiency at every measured time point. The highest removal efficiencies of lTCPEI(10K) were 82% and 77% for initial Au concentrations of 87.5 and 20.7 ppm, respectively, which indicates the decreasing efficiency with decreasing gold concentration. In contrast, lDCPEI(10K) maintained its removal efficiency of 94% at both lower concentrations. The dashed line is the straight line drawn from the final adsorption point and the earliest time point within a ±5% tolerance limit range is considered the equilibrium point. The circle pointed out the equilibrium points for the adsorbents. When C_0 = 584 ppm, lDCPEI(10K) reached equilibrium within 15 min whereas lTCPEI(10K) needed 30 min. At 87.5 and 20.7 ppm, lDCPEI(10K) reached equilibrium within 5 min, whereas lTCPEI(10K) required 15 and 5 min, respectively. The faster adsorption kinetics of DCPEI over TCPEI can be attributed to its longer rigid crosslinker length. TCT is smaller in size and it behaves as a compact crosslinking agent which creates short interchain bridges and a relatively tight network. In contrast, DTP is approximately three times larger, and it increases interchain spacing in the network, providing better accessibility of the bulky gold complex to the inner pores leading to faster kinetics. Adsorption phenomena of the second set of adsorbents, lDCPEI(1.8K) and lTCPEI(1.8K), were tested in three different initial gold concentrations same as the previous adsorbents set. For an initial gold concentration of 584 ppm, both adsorbents removed nearly 97% of gold from the solution, but lDCPEI(1.8K) reached adsorption equilibrium within 15 min, whereas lTCPEI(1.8K) required 30 min (SI-6a). Moreover, every point of the first 15 min of lDCPEI(10K) exhibited marginally higher adsorption capacity and efficiency. This trend is clearly demonstrated in the inset of SI-6a. lDCPEI(1.8K) exhibited gold adsorption efficiency of 87% and 91% at initial gold concentrations of 87.5 and 20.7 ppm, respectively, whereas lTCPEI(1.8K) showed a gold removal efficiency of around 75% in both cases (SI-6b,c). Further, when molecular weight (MW) of PEIs was taken into consideration, no significant change was observed in performance.

For 10 kDa molecular weight, gold removal efficiency was 98% for both adsorbents, and for 1.8 kDa, this removal efficiency was 96% and 97% (SI-6d). This indicates that the molecular weight of the backbone does not have a significant effect on the adsorption performance. Regenspurg et al. investigated two polyelectrolyte systems (PAH-PSS and PAH-PAA), and reported PAH-PSS molecular weight did not significantly affect the metal recovery performance.[34] A. Younis et al. reported that the MW of chitosan had no significant effect on removal of cadmium (Cd), whereas on Zn, Pb, Cu, it had noticeable influence.[35] In contrast, Geng et al. reported that in PEI crosslinked graphene oxide systems, metal recovery was highly dependent on molecular weight.[36] Notably, most of the previous MW-dependent metal recovery studies were conducted with membrane-based systems where MW can strongly influence polymer loading, layer thickness and membrane formation. Yet collectively, these studies indicate that the influence of polymer MW on metal recovery is case dependent and strongly governed by the material format, polymer accessibility, and mass-transport limitations.

3.2.2. Adsorption Kinetics. The adsorption kinetics were analyzed with two widely used, classical adsorption kinetics models, pseudo-first-order (PFO) (eq 12) and pseudo-second-order (PSO) (eq 13) adsorption kinetics models. These models helped to reveal both the nature and the rate of interactions. An initial gold concentration of 584 ppm was used for both

https://doi.org/10.1021/acssusresmgt.6c00020
ACS Sustain. Resour. Manag. 2026, 3, 1182−1191

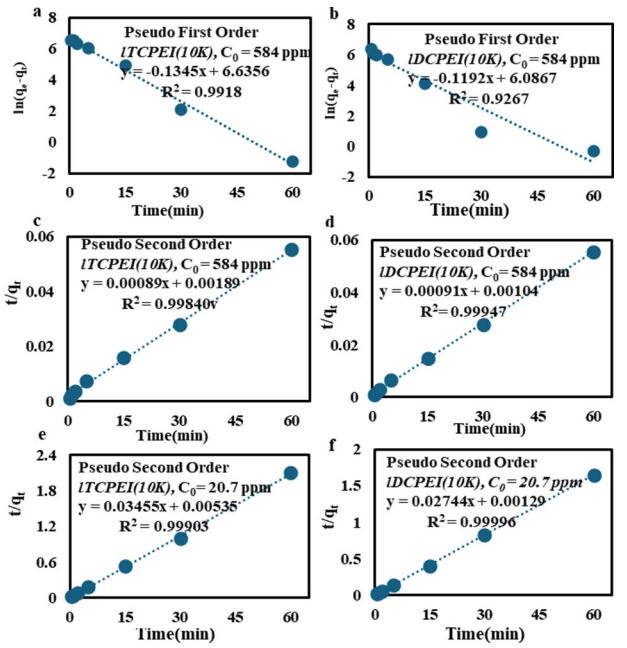

Figure 3. Pseudo-first-order and pseudo-second-order kinetics fitting results for lTCPEI and lDCPEI.

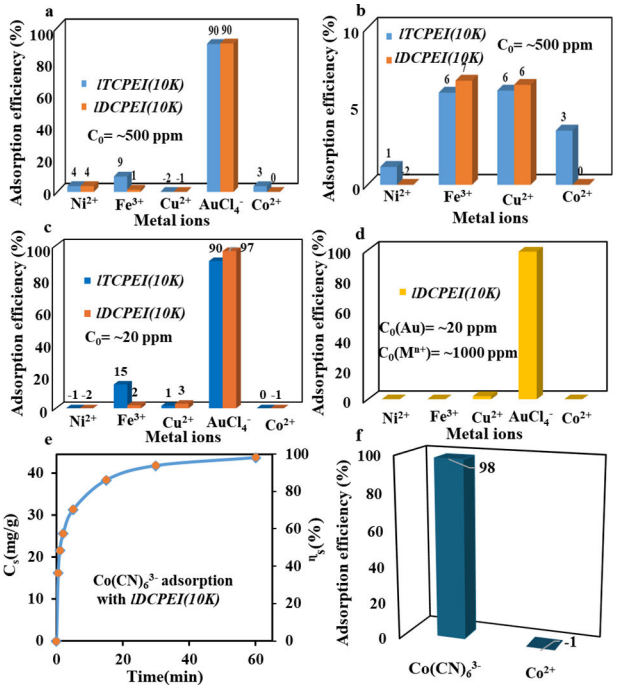

Figure 4. Adsorption efficiency of lTCPEI(10K) and lDCPEI(10K) for a mixed metal ion solution of ~500 ppm concentration for all metal ions (a) including gold or (b) in the absence of gold. (c) Adsorption efficiency of lTCPEI(10K) and lDCPEI(10K) for a mixed metal ion solution of ~20 ppm initial concentration for all metal ions, including gold. (d) Adsorption efficiency of lDCPEI(10K) for a mixed metal ion solution containing ~1000 ppm of other metals and ~20 ppm of gold. (e) $Co(CN)_6^{3-}$ adsorption with lDCPEI(10K). (f) Comparison between $Co(CN)_6^{3-}$ and Co^{2+} ions adsorption efficiency.

models. The PSO reaction model was also checked at a lower initial gold concentration of ~20 ppm. In Figure 3, linear plotting for PFO and PSO at C_0 = 584 and 20.7 ppm was shown. The pseudo-second-order model showed better fitting for both lTCPEI(10K) and lDCPEI(10K) with a higher correlation coefficient value (R^2 = 0.9984 and 0.9995, respectively) (SI-7 and Figure 3). Furthermore, the calculated equilibrium adsorbance capacity, (q_e) (lDCPEI = 1099 mg g^{-1}) also closely matched with the experimental equilibrium capacity (q_e) (lDCPEI = 1080 mg g^{-1}) for the pseudo-second-order reaction kinetics model (SI-7). Therefore, the adsorption follows a pseudo-second-order kinetic model, indicating that the sorption process is predominantly chemisorption.

Again, the pseudo-second-order model was checked with a lower initial gold concentration. At C_0 = 20.7 ppm, the correlation co-efficient was very close to 1 and the calculated q_es of 29 and 36 mg g^{-1} for lTCPEI and lDCPEI, respectively, which match close with the corresponding experimental values. The rate constant at this lower concentration was much higher (>500 times) than that at C_0 = 584 ppm. Compared to lTCPEI(10k) (k_2 = 0.2231 g mg^{-1} min^{-1}), lDCPEI(10k) (k_2 = 0.5837 g mg^{-1} min^{-1}) exhibited a 2.6 times higher pseudo-second-order rate constant, confirming faster adsorption kinetics for lDCPEI.

3.2.3. Selectivity Test and pH-Dependent Study. Acid leachates of e-waste contain various types of metal ions, predominantly copper, iron, cobalt, and nickel ions.[37] To assess selectivity, an initial experiment was performed with a mixed metal solution containing nearly 500 ppm of each ion. Both lTCPEI(10K) and lDCPEI(10K) selectively recovered 90% of gold from the solution with a minimal amount of other metal ions adsorbed (Figure 4a). This selectivity likely comes from electrostatic interaction between positively charged nitrogen atoms in the crosslinked polymers and the negatively charged gold complex.[38,39] In contrast, all other metal ions are positively charged, and the probable attractive interaction is coordination. Consequently, the removal efficiency of these metals was very low. Due to the rapid nature of electrostatic interaction, gold ions might quickly occupy most of the active sites of the adsorbents leaving no room for other metal ions to coordinate. To validate this, another experiment was conducted with a new mixed metal ion solution without gold. As shown in Figure 4b, the highest removal efficiency among those metals was 7% after 1 h contact time. This indicates that, in the absence of gold, CPEIs still showed very little affinity for the positively charged metal ions. Additional experiments were conducted with a metal ion solution of ~20 ppm to access adsorption behavior at very low concentrations. At this concentration, both adsorbents recovered more than 90% of gold again from the solutions with only small amount of other metals recovered (Figure 4c). In real-life acid leachates of e-waste, the concentrations of copper, iron and other metals are typically much higher than gold.[37]

To mimic this condition, the gold concentration was kept at around 20 ppm, while other metal concentrations were increased to approximately 1000 ppm. As shown in Figure 4d, it was clearly confirmed that even in the presence of significantly higher concentrations of competing metal ions, the lDCPEI(10K) was able to recover gold selectively. To confirm that selectivity is primarily driven by electrostatic interactions, potassium hexacyanocobaltate (III) was used as a test salt where $Co(CN)_6^{3-}$ was a stable complex ion. The initial concentration of cobalt was approximately 20 ppm and lDCPEI(10K) was used as an adsorbent. As shown in Figure 4e, most of the cobalt was recovered from the solution within 1 h, obtaining 98% adsorption efficiency. In contrast, the previously tested same concentration of Co^{2+} ion

https://doi.org/10.1021/acssusresmgt.6c00020
ACS Sustain. Resour. Manag. 2026, 3, 1182−1191

exhibited very minimal adsorption efficiency, further supporting the dominating role of electrostatic interactions (Figure 4f).

The zeta potentials of both lDCPEI(10K) and lTCPEI(10K) were measured over an appropriate pH range (SI-8a). Both crosslinked polymers exhibited positive zeta potential through pH 2–10 and isoelectric points (IEP) were 10.75 and 10.95, respectively. These results suggest that there are positively charged protonated amine groups up to pH = 10 to facilitate gold recovery. Further adsorption studies of lDCPEI(10K) were conducted under different pH because electrostatic interaction is expected to play a vital role for $[AuCl_4]^-$ uptake. The pH-dependent study was carried out with an initial gold concentration of ~20 ppm, and a contact time was maintained at 30 min. The recovery tests were conducted with three separate samples at each pH with a standard deviation-based error bar confirming reproducibility (SI-8b). At pH 2.0 and 5.0, gold recovery remained nearly constant at ~95%. The recovery efficiency decreased to 84% at pH = 7.0 and continued to decline with increasing pH, and down to 64% at pH = 11.0. From these studies, pH 2–5 is identified as the optimized pH range for gold adsorption, where consistently high recovery can be achieved.

3.2.4. Adsorption Isotherm. Equilibrium adsorption capacity (q_e) was investigated over initial gold concentration to determine the maximum adsorption capacity and adsorption behaviors. Both adsorbents showed similar phenomena and reached maximum adsorption capacity at 3000 ppm initial gold concentration. With increasing initial gold concentration, equilibrium adsorption capacity also increased proportionally up to 3000 ppm after which the curve becomes a plateau (Figure 5a). To reduce each Au^{3+} ion, at least three nitrogen atoms are required. A plot of stoichiometrically estimated nitrogen to absorbed gold molar ratio versus initial gold concentration showed that at saturated conditions, the number of nitrogen atoms was approximately twice compared to gold molecules (Figure 5b). This indicates that not all gold complexes could be reduced, and some remained as the $AuCl^{4-}$ complex. Three popular adsorption isotherm models were applied to acquire deeper insights into the sorption process. These models were the Langmuir, the Freundlich, and the Dubinin–Radushkevich (D–R) isotherm models. Linear equations for these models were represented by eqs 4, 7, and 10, respectively. The linear plotting of these models for lTCPEI(10K) and lDCPEI(10K) is exhibited in Figure 5c–h, and the findings from the isotherm models are shown in SI-9. The Langmuir isotherm model showed the best fit for both adsorbents with R^2 values of 0.99956 and 0.99856 for lTCPEI(10K) and lDCPEI(10K), respectively (Figure 5 and SI-9). This suggests monolayer adsorption on a homogeneous surface. Maximum adsorption capacities were calculated from this isotherm model to be 2857 and 2777 mg/g for lTCPEI(10K) and lDCPEI(10K), respectively. Dimensionless separation factors (R_L) were calculated from the Langmuir constant according to eq 5. The R_L value is between 0 and 1 for both adsorbents, indicating a favorable adsorption process. This suggests that the adsorbent had a strong affinity toward adsorbate and adsorption happened spontaneously. Comparison with the recent literature indicates that these results rank among the highest in terms of maximum adsorption capacity and removal efficiency for adsorbents of gold (SI-10). Although Freundlich and D–R isotherm models showed not as good agreement with the experimental data, adsorption intensity and free energy were still calculated from those fittings. Adsorption intensity, n, was calculated from the slope of the linear regression of the Freundlich isotherm

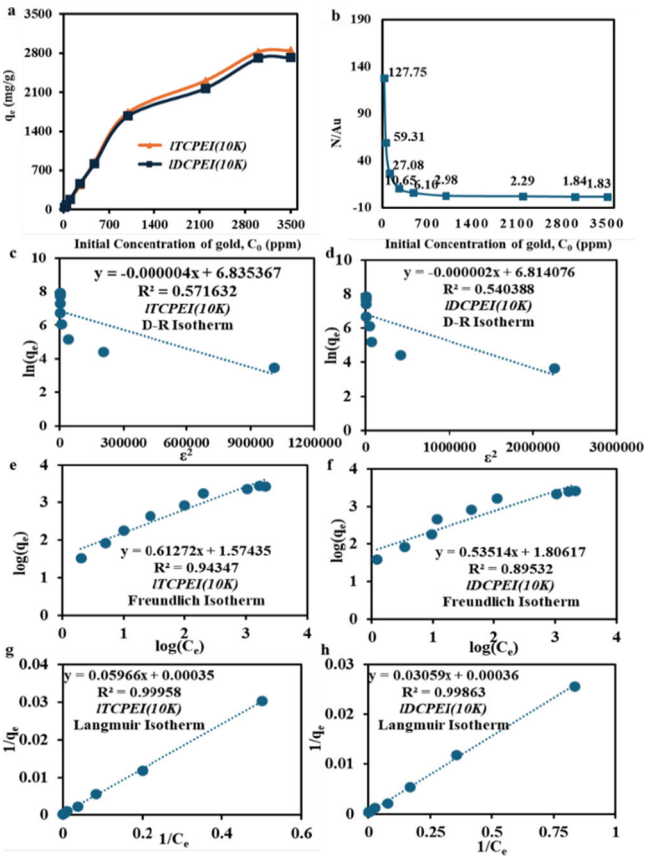

Figure 5. (a) Adsorption capacity vs initial gold concentration. (b) Mole ratio of nitrogen to gold vs gold concentration. (c–h) Linear fitting of isotherm models for lTCPEI(10K) and lDCPEI(10K).

models. Both adsorbents showed an 'n' value greater than 1, which indicates a favorable adsorption process, consistent with the Langmuir isotherm model.

From the D–R isotherm model, another important parameter, free energy of adsorption, E, was determined. For lTCPEI(10K) and lDCPEI(10K), E values were calculated to be 353 and 500 KJ/mole, respectively, both of which are much higher than 8 KJ/mole, indicating that a chemisorption process predominates. This interpretation is consistent with previously reported amine-based or nitrogen-rich sorbent where Au(III) uptake is largely governed by strong chemical interactions.[40−42]

3.2.5. Adsorption Mechanism. Linear polyethyleneimine contains repeating secondary amines in its backbone along with two terminal primary amines. At physiological pH ~7.4, about 55% of the amine groups are reported to be protonated for secondary amines.[43] The pH values of the 584 ppm and 20 ppm $HAuCl_4$ solutions were measured to be 2.23 and 3.23, respectively. At such an acidic pH, most of the amine groups of linear PEIs were expected to be protonated, resulting in a highly positively charged polymer. Therefore, electrostatic attraction between these positively charged, protonated amines and the negatively charged $AuCl^{4-}$ presumably dominated the adsorption mechanism. To validate this assumption, $Co(CN)_6^{3-}$ was selected as an alternative negative complex, briefly discussed in the selectivity section. Figure 4f clearly shows that electrostatic attraction was one of the major interactions between CPEIs and the gold complex. To investigate further, powder XRD analysis was performed. Before gold adsorption, there was only one broad polymer peak

https://doi.org/10.1021/acssusresmgt.6c00020
ACS Sustain. Resour. Manag. 2026, 3, 1182−1191

around 20.9°. After gold adsorption for 1 h, five sharp peaks were observed well matching with the metallic gold peaks.[44] After desorption, these peaks disappeared, leaving a broad polymer peak (SI-11a). This suggests that, although gold was initially adsorbed as $AuCl^{4-}$ complex ion to the CPEIs, eventually it was reduced to metallic gold and the thiourea solution can redissolve that metallic gold. In this process, amine groups in lPEI are oxidized to imine or enamine groups and lose electrons. Oxidation of amine groups and concurrent reduction of gold were supported by the previous literature.[44−46] FTIR spectra of lDCPEI(10K) after gold adsorption exhibited a new specific peak of C=N at 1600 cm^{-1} after gold adsorption, confirming the oxidation process of amine groups (SI-11b). After desorption of gold, C=N peaks remained, indicating that all oxidized imines could not go back to their original state.

A systematic study on adsorbent and gold was performed with powder XRD (pXRD) to provide more insights into gold reduction. Gold solutions with the adsorbents were stirred for a certain amount of time, i.e., 7 min, 1 h, and 24 h and then filtered and vacuum dried before pXRD testing. Figure 6a shows that the gold peak intensity increases with increasing stirring time of adsorbent lDCPEI(10K) in solution. The gold adsorption efficiency of this solution was measured and as expected 97% of gold was adsorbed within the first 7 min. However, the intensity of metallic gold peaks in pXRD was very minimal. Assuming the intensity of the most prominent peak at $2\theta = 38.1°$ representing 100% gold reduction after 24 h, only 0.52% of gold was reduced within the first 7 min and 53.09% after the first 1 h (SI-12). Similar behavior was observed with lTCPEI(10K) (Figure 6b). This clearly indicates that gold adsorption occurred rapidly through electrostatic interaction within the pores of adsorbents, followed by slow reduction of Au(III) to metallic gold over a period of 24 h. Since most of the gold was adsorbed within the first 7 min, it raises the question whether the reduction still occurs if the adsorbent was filtered immediately after 7 min and stored in a solid state for a longer time. Figure 6c,d suggests that gold reduction was also continued in the solid state but at a much slower rate than in solution. Compared to the previous 24 h solution state, lDCPEI(10K) showed only a little increase from 0.52 to 3.42% after being stored for 1 week in the solid state (SI-12). SEM analysis was performed on lDCPEI(10K) before and after gold adsorption. The initial SEM image of adsorbent lDCPEI(10K), Figure 6e reveals its porous morphology. After 7 min of adsorption, small-sized gold particles were observed on the surface (Figure 6f). Gold particles grew larger, and the number of particles also increased significantly after 1 h in gold solution due to aggregation and reduction of a significant amount of gold complex (Figure 6g). After gold desorption, the original porous structure of lDCPEI(10K) was restored, as shown in Figure 6h. Further confirmation came from energy-dispersive X-ray spectroscopy (EDS). Elemental analysis showed that lDCPEI(10K) possessed 21.61 wt % of gold post adsorption (SI-13a,b), and elemental mapping indicates a homogeneous distribution of gold (SI-14). This further confirmed that gold is adsorbed across the porous morphology of CPEIs.

3.2.6. Desorption Study. A desorption study was performed with both adsorbents, and the initial concentration of gold was 20 ppm. 5% thiourea solution in 3 M hydrochloric acid was used as the desorption agent. Gold desorption in thiourea solution was very fast. As shown in SI-15a, within the

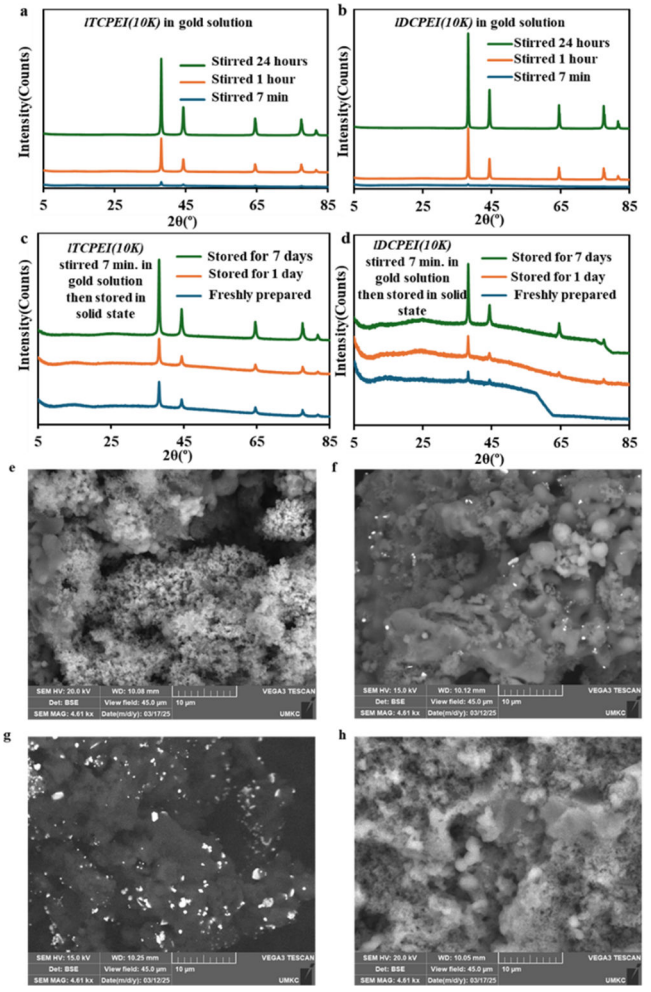

Figure 6. pXRD analysis data on lTCPEI and lDCPEI, (a,b) stirred in gold solution for different amounts of time. (c,d) After stirred for 7 min in gold solution, samples were filtered and stored in solid state. SEM images of lDCPEI(10K) (e) before gold adsorption, (f) after 7 min gold adsorption, (g) after 1 h gold adsorption, and (h) after gold desorption.

first 30 s, gold desorption from lDCPEI(10K) was completed. Both adsorbents successfully released ∼100% of the adsorbed gold within a 5-min time frame (SI-15b). Almost 96% of gold was recovered from lTCPEI(10K), and 100% of gold was reclaimed from lDCPEI(10K). To check the regeneration ability, adsorption and desorption were repeated in five consecutive cycles. The desorption efficiencies remained consistently near 100%, indicating that the desorption agent effectively removed Au particles from binding sites after multiple cycles (SI-16b). However, the adsorption efficiencies decreased gradually with each reuse cycle. After five consecutive cycles, it decreased to 75% (SI-16a). Notably, it retained >80% recovery efficiency after three consecutive cycles. After adsorption, the reduction of Au (III) to Au (0) likely occurred, accompanied by oxidation of some C–N functionalities to C=N species (SI-11b). FTIR data analysis of lDCPEI(10K) after desorption suggested that some imine moieties could not go back to their original state, reducing the availability of active nitrogen binding sites and likely contributing to diminishing the adsorption performance (SI-11b). However, it retained >85% of its initial recovery efficiency after three consecutive cycles. Reusing the same adsorbent in multiple cycles directly

https://doi.org/10.1021/acssusresmgt.6c00020
ACS Sustain. Resour. Manag. 2026, 3, 1182−1191

quantifies as reducing material consumption. The adsorptions and desorption cycles were conducted predominantly with acidic aqueous media. While a full life cycle assessment is beyond the scope of this study, these results indicate multicycle reuse with limited non aqueous solvent demand.

4. CONCLUSIONS

A comparative kinetic study was conducted using four newly synthesized crosslinked polymers prepared with two crosslinkers of different sizes and linear PEI with two different molecular weights, 10 and 1.8 kDa. All crosslinked adsorbents with different size of crosslinkers successfully removed most of the gold from simulated e-waste, whereas detailed adsorption studies revealed that lDCPEI(10K) completed adsorption and reached equilibrium faster than lTCPEI(10K). Comparable behavior was observed with the 10K and 1.8K variants across three different initial gold concentrations, further strengthening the claims. The pseudo-second-order adsorption kinetics model gave the best fit and the rection rate constant calculated from this model for lDCPEI(10K) was about double that for the lTCPEI(10K). Both adsorbents selectively and effectively removed gold from the solution containing multiple competing metal ions typically found in e-waste. This remarkable selectivity comes from the electrostatic interaction of the gold complex with adsorbents. 5% thiourea solution in HCl efficiently separated gold from adsorbents. Desorption was rapid, and nearly 96–100% of gold was released within the first 30 s and up to three reuse cycles the recovery efficiency retained more than 80%. The Langmuir isotherm model exhibited excellent fitting, confirming a monolayer adsorption mechanism. The adsorption is primarily due to electrostatic interactions, followed by a redox process occurring on the adsorbent surfaces. Based on these observations, these excellent adsorbents demonstrate strong potential for practical implementation in real-world gold recovery systems. Their effectiveness will be further evaluated using actual e-waste in forthcoming studies. The adsorbents will also be assessed under process-relevant conditions, such as continuous-flow or packed bed column configurations. These studies will provide a more rigorous validation of selectivity and robustness and strengthen the relevance of the material's practical implementation. In addition, future focus will be on expanding this crosslinked materials strategy beyond Au(III) to other precious and critical metals particularly Pt, Rh, and Ir, where selective capture from complex leachate remains challenging.

■ ASSOCIATED CONTENT

Supporting Information

The Supporting Information is available free of charge at https://pubs.acs.org/doi/10.1021/acssusresmgt.6c00020.

Details of the adsorption experiments and the equations used to analyze the result; structures of polymers and crosslinkers along with reaction scheme; solid state NMR and FTIR; overall process flow chart and gold recovery data comparison for CPEIs(1.8K); adsorption kinetics and isotherms data table; summarized data on recently published articles and cost details of our crosslinkers; desorption study along with consecutive adsorption and desorption cycle performance for crosslinked polymers; powder XRD and EDS data of CPEIs before and after gold adsorption; and TGA analysis data (DOCX)

■ AUTHOR INFORMATION

Corresponding Authors

Peng Tao − *Department of Chemistry, and O'Donnell Data Science and Research Computing Institute, Southern Methodist University, Dallas, Texas 75205, USA;* orcid.org/0000-0002-2488-0239; Email: ptao@mail.smu.edu

Zhonghua Peng − *Division of Energy, Matter and Systems, School of Science and Engineering, University of Missouri-Kansas City, Kansas City, Missouri 64110, USA;* Email: pengz@umkc.edu

Xiaobo Chen − *Division of Energy, Matter and Systems, School of Science and Engineering, University of Missouri-Kansas City, Kansas City, Missouri 64110, USA;* orcid.org/0000-0002-7127-4813; Email: chenxiaobo@umkc.edu

Authors

Syfur R. Tushar − *Division of Energy, Matter and Systems, School of Science and Engineering, University of Missouri-Kansas City, Kansas City, Missouri 64110, USA;* orcid.org/0009-0003-8455-3285

Yong Li − *Division of Energy, Matter and Systems, School of Science and Engineering, University of Missouri-Kansas City, Kansas City, Missouri 64110, USA*

James Murowchick − *Division of Energy, Matter and Systems, School of Science and Engineering, University of Missouri-Kansas City, Kansas City, Missouri 64110, USA;* orcid.org/0000-0003-2987-0352

Todor Gounev − *Division of Energy, Matter and Systems, School of Science and Engineering, University of Missouri-Kansas City, Kansas City, Missouri 64110, USA*

Nafisa Tasnim − *Division of Energy, Matter and Systems, School of Science and Engineering, University of Missouri-Kansas City, Kansas City, Missouri 64110, USA;* orcid.org/0009-0005-5085-202X

Sai Siva Kumar Pinnepalli − *Division of Energy, Matter and Systems, School of Science and Engineering, University of Missouri-Kansas City, Kansas City, Missouri 64110, USA;* Present Addresses: Technology Research, Intel Corporation, Hillsboro, Oregon, USA.

Complete contact information is available at: https://pubs.acs.org/doi/10.1021/acssusresmgt.6c00020

Author Contributions

S.R.T.: Methodology; investigation; data collection; formal analysis; visualization; writing—original draft. Y.L.: Instrument set-up and user training, review and editing draft. J.M.: Instrument training for user and data curation for XRD, SEM, and EDS. T.G.: Initial instrument training and troubleshooting, methodology development for AAS. N.T.: Acquired partial AAS and FTIR data; interpreted AAS/FTIR results. S.S.K.P.: Acquiring and analyzing solid state NMR. P.T.: Funding acquisition, review and editing draft. X.C.: Funding acquisition, review and editing draft. Z.P.: Supervision, funding acquisition,

https://doi.org/10.1021/acssusresmgt.6c00020
ACS Sustain. Resour. Manag. 2026, 3, 1182−1191

review and editing draft. All authors contributed to the discussion of results and approved the final manuscript.

Notes

The authors declare no competing financial interest.

■ ACKNOWLEDGMENTS

The authors acknowledge the National Science Foundation (NSF) for funding this project (NSF CBET-2315087).

■ ABBREVIATIONS

TCT	2,46-trichloror-1,3,5-triazine
lTCPEI	triazine crosslinked linear polyethyleneimine
DTP	di-triazine piperazine
lDCPEI	DTP crosslinked linear polyethyleneimine
CPEI	crosslinked polyethyleneimine

■ REFERENCES

(1) *Tackling Informality in E-Waste Management*: *The Potential of Cooperative Enterprises*; Official website; Internatinal Labour Organization: Geneva, **2014**.

(2) *Electronic Waste* (*e-Waste*); Official website; WHO: **2024**.

(3) *Global E-Waste Monitor 2024*: *Electronic Waste Rising Five Times Faster than Documented E-Waste Recycling*; Official websitr; UNITAR: Geneva, **2024**.

(4) Rao, M. D.; Singh, K. K.; Morrison, C. A.; Love, J. B. Challenges and Opportunities in the Recovery of Gold from Electronic Waste. *RSC Adv.* **2020**, *10* (8), 4300–4309.

(5) Gopikrishnan, V.; Vignesh, A.; Radhakrishnan, M.; Joseph, J.; Shanmugasundaram, T.; Doble, M.; Balagurunathan, R. Microbial Leaching of Heavy Metals from E-Waste *Biovalorisation of Wastes to Renewable Chemicals and Biofuels* Elsevier **2020**, 189–216.

(6) Huy Do, M.; Tien Nguyen, G.; Dong Thach, U.; Lee, Y.; Huu Bui, T. Advances in Hydrometallurgical Approaches for Gold Recovery from E-Waste: A Comprehensive Review and Perspectives. *Miner. Eng.* **2023**, *191*, No. 107977.

(7) Chakraborty, S. C.; Qamruzzaman, M.; Zaman, M. W. U.; Alam, M. M.; Hossain, M. D.; Pramanik, B. K.; Nguyen, L. N.; Nghiem, L. D.; Ahmed, M. F.; Zhou, J. L.; Ibrahim Mondal, M. d.; Hossain, M. A.; Johir, M. A. H.; Ahmed, M. B.; Sithi, J. A.; Zargar, M.; Moni, M. A. Metals in E-Waste: Occurrence, Fate, Impacts and Remediation Technologies. *Process Saf. Environ. Prot.* **2022**, *162*, 230–252.

(8) Ankit, Saha, L.; Kumar, V.; Tiwari, J.; Sweta, Rawat, S.; Singh, J.; Bauddh, K. Electronic Waste and Their Leachates Impact on Human Health and Environment: Global Ecological Threat and Management. *Environ. Technol. Innov.* **2021**, *24*, No. 102049.

(9) Pinto, V. E-Waste Hazard: The Impending Challenge. *Indian J. Occup. Environ. Med.* **2008**, *12* (2), 65.

(10) Ahirwar, R.; Tripathi, A. K. E-Waste Management: A Review of Recycling Process, Environmental and Occupational Health Hazards, and Potential Solutions. *Environ. Nanotechnol. Monit. Manage.* **2021**, *15*, No. 100409.

(11) Ahmad, M.; Shah, T.; Tariq, M. R.; Zhang, L.; Lyu, Y.; Iqbal, W.; Naik, M. U.-D.; Khosla, A.; Zhang, Q.; Zhang, B. Recent Trends in Material Design and Preparation with Structure-Activity Relationship for Gold Recovery from E-Waste: A Review. *J. Cleaner Prod.* **2023**, *426*, No. 139012.

(12) Cotton, S. A. *Chemistry of Precious Metals*; Blackie Academic & Professional: **1997**.

(13) *Gold Demand Trends Q1 2024*; World Gold Council: 2024.

(14) Shang, H.; Chen, Y.; Guan, S.; Wang, Y.; Cao, J.; Wang, X.; Li, H.; Bian, Z. Scalable and Selective Gold Recovery from End-of-Life Electronics. *Nat. Chem. Eng.* **2024**, *1* (2), 170–179.

(15) Goodman, P. Current and Future Uses of Gold in Electronics. *Gold Bull.* **2002**, *35* (1), 21–26.

(16) *Precious Metals E-Waste Recovery Market* (*2024 - 2030*); GVR-4-68040-223-5; Grand View Report; p 104.

(17) Nogueira, A. F. M.; Carreira, A. R. F.; Vargas, S. J R; Passos, H.; Schaeffer, N.; Coutinho, J. A. P. Simple Gold Recovery from E-Waste Leachate by Selective Precipitation Using a Quaternary Ammonium Salt. *Sep. Purif. Technol.* **2023**, *316*, No. 123797.

(18) Murakami, H.; Nishihama, S.; Yoshizuka, K. Separation and Recovery of Gold from Waste LED Using Ion Exchange Method. *Hydrometallurgy* **2015**, *157*, 194–198.

(19) Vojoudi, H.; Badiei, A.; Banaei, A.; Bahar, S.; Karimi, S.; Mohammadi Ziarani, G.; Ganjali, M. R. Extraction of Gold, Palladium and Silver Ions Using Organically Modified Silica-Coated Magnetic Nanoparticles and Silica Gel as a Sorbent. *Microchim. Acta* **2017**, *184* (10), 3859–3866.

(20) Argiropoulos, G.; Cattrall, R. W.; Hamilton, I. C.; Kolev, S. D.; Paimin, R. The Study of a Membrane for Extracting Gold(III) from Hydrochloric Acid Solutions. *J. Membr. Sci.* **1998**, *138* (2), 279–285.

(21) Zhou, S.; Mo, X.; Zhu, W.; Xu, W.; Tang, K.; Lei, Y. Selective Adsorption of Au(III) with Ultra-Fast Kinetics by a New Metal-Organic Polymer. *J. Mol. Liq.* **2020**, *319*, No. 114125.

(22) Deng, K.; Yin, P.; Liu, X.; Tang, Q.; Qu, R. Modeling, Analysis and Optimization of Adsorption Parameters of Au(III) Using Low-Cost Agricultural Residuals Buckwheat Hulls. *J. Ind. Eng. Chem.* **2014**, *20* (4), 2428–2438.

(23) Xu, W.; Wang, F.; Chen, S.; Zhang, K.; Tang, K. Efficient and Selective Recovery of Gold and Palladium by Simple and Easily Synthesized Polyethylenimine Based Polymer. *Sep. Purif. Technol.* **2024**, *328*, No. 125039.

(24) Zhang, Z.; Xu, W.; Zhang, K.; Tang, K. Highly Efficient and Fast Adsorption of Au(III) and Pd(II) by Crosslinked Polyethyleneimine-glutaraldehyde. *AIChE J.* **2023**, *69* (3), No. e17950.

(25) Liu, F.; Zhou, L.; Wang, W.; Yu, G.; Deng, S. Adsorptive Recovery of Au(III) from Aqueous Solution Using Crosslinked Polyethyleneimine Resins. *Chemosphere* **2020**, *241*, No. 125122.

(26) Lin, X.; Tran, D. T.; Song, M.-H.; Yun, Y.-S. Development of Polyethyleneimine-Starch Fibers Stable over the Broad pH Range for Selective Adsorption of Gold from Actual Leachate Solutions of Waste Electrical and Electronic Equipment. *J. Cleaner Prod.* **2021**, *328*, No. 129545.

(27) Hu, B.; Yang, M.; Huang, H.; Song, Z.; Tao, P.; Wu, Y.; Tang, K.; Chen, X.; Yang, C. Triazine-Crosslinked Polyethyleneimine for Efficient Adsorption and Recovery of Gold from Wastewater. *J. Mol. Liq.* **2022**, *367*, No. 120586.

(28) Steffensen, M. B.; Simanek, E. E. Chemoselective Building Blocks for Dendrimers from Relative Reactivity Data. *Org. Lett.* **2003**, *5* (13), 2359–2361.

(29) Patel, H. A.; Karadas, F.; Canlier, A.; Park, J.; Deniz, E.; Jung, Y.; Atilhan, M.; Yavuz, C. T. High Capacity Carbon Dioxide Adsorption by Inexpensive Covalent Organic Polymers. *J. Mater. Chem.* **2012**, *22* (17), 8431.

(30) Altarawneh, S. S. Combustion Characteristics and Thermal Degradation Kinetics of Microporous Triazine-Based Organic Polymers: The Role of Organic Linkers. *Polym. Bull.* **2024**, *81* (17), 15791–15821.

(31) Bhattacharyya, A. S.; Kumar, S.; Sharma, A.; Kumar, D.; Patel, S. B.; Paul, D.; Dutta, P. P.; Bhattacharjee, G. Metallization and APPJ Treatment of Bismaleimide. *High Perform. Polym.* **2017**, *29* (7), 816–826.

(32) Aghahosseini, H.; Rezaei, S. J. T.; Abdolahnjadian, D.; Maleki, M.; Ramazani, A. Ag–Pd Alloy Immobilized on Semi-Heterogeneous Support as a Novel Highly Efficient Artificial Nitroreductase: Experimental Design Optimization and Kinetic Study. *Catal. Lett.* **2021**, *151* (5), 1262–1272.

(33) Mokhtari, N.; Dinari, M.; Rahmanian, O. Novel Porous Organic Triazine-based Polyimide with High Nitrogen Levels for Highly Efficient Removal of Ni(II) from Aqueous Solution. *Polym. Int.* **2019**, *68* (6), 1178–1185.

https://doi.org/10.1021/acssusresmgt.6c00020
ACS Sustain. Resour. Manag. 2026, 3, 1182–1191

(34) Regenspurg, J. A.; Martins Costa, A. F.; Achterhuis, I.; De Vos, W. M. Influence of Molecular Weight on the Performance of Polyelectrolyte Multilayer Nanofiltration Membranes. *ACS Appl. Polym. Mater.* **2022**, *4* (5), 2962–2971.
(35) Younis, M.; Aly-Eldeen, M. A.; Elkady, E. M. Effect of Different Molecular Weights of Chitosan on the Removal Efficiencies of Heavy Metals from Contaminated Water. *Egypt. J. Aquatic Biol. Fish.* **2019**, *23* (4), 149–158.
(36) Geng, J.; Yin, Y.; Liang, Q.; Zhu, Z.; Luo, H. Polyethyleneimine Cross-Linked Graphene Oxide for Removing Hazardous Hexavalent Chromium: Adsorption Performance and Mechanism. *Chem. Eng. J.* **2019**, *361*, 1497–1510.
(37) He, Y.; Hosseinzadeh-Bandbafha, H.; Kiehbadroudinezhad, M.; Peng, W.; Tabatabaei, M.; Aghbashlo, M. Environmental Footprint Analysis of Gold Recycling from Electronic Waste: A Comparative Life Cycle Analysis. *J. Cleaner Prod.* **2023**, *432*, No. 139675.
(38) Dangi, Y. R.; Bediako, J. K.; Lin, X.; Choi, J.-W.; Lim, C.-R.; Song, M.-H.; Han, M.; Yun, Y.-S. Polyethyleneimine Impregnated Alginate Capsule as a High Capacity Sorbent for the Recovery of Monovalent and Trivalent Gold. *Sci. Rep.* **2021**, *11* (1), 17836.
(39) An, F.-Q.; Li, M.; Wu, R.-Y.; Hu, T.-P.; Gao, J.-F.; Yuan, Z.-G. Effective Recovery of $AuCl_4^-$ Using D301 Resin Functionalized with Ethylenediamine and Thiourea. *Hydrometallurgy* **2017**, *169*, 356–361.
(40) Samadi, A.; Kong, L.; Guo, W.; Sillanpää, M.; Boztepe, I.; Song, C.; Zeng, Q.; Zhao, S. Standardized Methodology for Performance Evaluation in Using Polyaniline-Based Adsorbents to Remove Aqueous Contaminants. *J. Environ. Chem. Eng.* **2024**, *12* (3), No. 112650.
(41) Huang, C.; Xu, X.; Ao, J.; Ma, L.; Ye, F.; Wang, Z.; Xu, L.; Zhao, X.; Ma, H. Selective Adsorption, Reduction, and Separation of Au(III) from Aqueous Solution with Amine-Type Non-Woven Fabric Adsorbents. *Materials* **2020**, *13* (13), 2958.
(42) He, H.; Yang, X.; Li, S.; Xu, Y.; Ye, S.; Xiong, M.; Yang, N.; Feng, C.; Zhang, Y.; Nie, Z. Quaternary Amine-Functionalized Electrospun Nanofibers for Selective Gold Capture: Experimental and DFT Calculation Study. *Sep. Purif. Technol.* **2025**, *376*, No. 133945.
(43) Ziebarth, J. D.; Wang, Y. Understanding the Protonation Behavior of Linear Polyethylenimine in Solutions through Monte Carlo Simulations. *Biomacromolecules* **2010**, *11* (1), 29–38.
(44) Lee, K. Y.; Hwang, J.; Lee, Y. W.; Kim, J.; Han, S. W. One-Step Synthesis of Gold Nanoparticles Using Azacryptand and Their Applications in SERS and Catalysis. *J. Colloid Interface Sci.* **2007**, *316* (2), 476–481.
(45) Bali, K.; Bak, M.; Szarka, K.; Juhász, G.; Sáfrán, G.; Pécz, B.; Mihály, J.; Mészáros, R. Controlling the Morphology of Poly(Ethyleneimine)/Gold Nanoassemblies through the Variation of pH and Electrolyte Additives. *J. Mol. Liq.* **2021**, *322*, No. 114559.
(46) Kuo, P.-L.; Chen, C.-C.; Jao, M.-W. Effects of Polymer Micelles of Alkylated Polyethylenimines on Generation of Gold Nanoparticles. *J. Phys. Chem. B* **2005**, *109* (19), 9445–9450.

https://doi.org/10.1021/acssusresmgt.6c00020
ACS Sustain. Resour. Manag. 2026, 3, 1182–1191